$CoFe_2O_4$/CHITOSAN MAGNETIC NANOCOMPOSITE: SYNTHESIS, CHARACTERIZATION AND APPLICATION FOR ADSORPTION OF ACIDIC YELLOW DYE FROM AQUEOUS SOLUTIONS

HAMIDREZA ANSARI, MAHSASADAT MIRALINAGHI and FARIBORZ AZIZINEZHAD

Department of Chemistry, Faculty of Science, Islamic Azad University, Varamin-Pishva Branch, P.O. Box 33817-7489, Varamin, Iran

✉ *Corresponding author: M. Miralinaghi, m_miralinaghi@iauvaramin.ac.ir*

Received July 7, 2018

Magnetic chitosan-modified $CoFe_2O_4$ nanoparticles, CS/$CoFe_2O_4$, were successfully synthesized by an *in situ* coprecipitation technique. The structure, crystal phase, surface morphology and magnetic properties of CS/$CoFe_2O_4$ were characterized by FTIR, TGA, XRD, FE-SEM, EDX and VSM analyses. The as-prepared CS/$CoFe_2O_4$ nanoparticles were employed to adsorb Acid Yellow 17 dye (AY17) from aqueous solutions. The influence of experimental parameters, such as pH, temperature, contact time, adsorbent dosage and initial dye concentration on the efficiency of AY17 adsorption was studied. The maximum dye removal percentage reached 90% after 90 min adsorption at pH 4.0 and 323 K for the solution with an initial AY17 concentration of 30 mg L^{-1} and CS/$CoFe_2O_4$ dose of 0.01 g. The adsorption kinetics agreed well with the pseudo-second order model. The isothermal data preferably followed the Langmuir model, with the maximum adsorption capacity of 89.10 mg g^{-1}. Thermodynamic studies illustrated that the adsorption process is endothermic and spontaneous.

Keywords: Acid yellow, adsorption, chitosan, dye, removal

INTRODUCTION

Dyes are colored organic compounds, extensively used to impart color to raw materials and applied in the production of leather, paper, pharmaceuticals, foods, cosmetics, plastics, textiles *etc.*[1] More than 10000 tons of dye are annually used only in the textile industry worldwide and almost 100 tons of dyes are discharged into waste streams per year.[2] A huge number of industrial dyes are highly toxic, carcinogenic and mutagenic, even at relatively low concentrations, causing serious environmental hazards and severe damage to humans. The removal of dyes from effluents plays a crucial role in controlling water pollution and conserving aquatic ecosystems.[3] Among the range of techniques available for dye removal from effluents, adsorption is recognized as a simple, efficient and economical technique used for wastewater treatment, especially in less developed countries. Undoubtedly, due to its high porosity and huge surface area (200-500 m^2g^{-1}), active carbon is the most common adsorbent applied in dye adsorption, but its high cost and low regeneration limit its application. Therefore, further research is necessary to develop novel absorbents that are economically cost-effective and environmentally friendly, besides being capable of removing a huge amount of pollutants, and being easily and rapidly recovered.[4,5]

Due to their high number of surface-active sites, fast removal rates and easy magnetic recovery, magnetic nanoparticles have emerged as promising absorbents, compared to traditional ones.[6,7] However, magnetic nanoparticles are chemically highly active and easily oxidized in the air, affecting the long-term magnetic performance and applicability of the separation process. In addition, magnetic interactions between naked nanoparticles make them capable of rapid and uncontrolled accumulation under normal synthesis conditions. The most appropriate strategy to stabilize magnetic nanoparticles against oxidation, corrosion and spontaneous accumulation is coating them with organic or mineral materials.[8,9] Natural organic macromolecules, mostly biopolymers, such as

chitin, chitosan (CS), cyclodextrin, alginate *etc*., are used as effective coatings, covering very well these particles.[10-12]

In this research, the CS/$CoFe_2O_4$ composite was prepared and its structural specifications were characterized. The adsorption properties of the CS/$CoFe_2O_4$ composite towards the AY17 dye (as a function of pH, temperature, contact time, amount of CS/$CoFe_2O_4$ and the initial dye concentration) were studied using batch tests. Also, the mechanism of the interaction between AY17 and the prepared composite was discussed. Furthermore, the kinetic parameters, equilibrium isotherms and thermodynamics were determined.

EXPERIMENTAL

Materials

Acid Yellow 17 (chemical formula $C_{16}H_{10}Cl_2N_4Na_2O_7S_2$, FW = 551.29 g mol^{-1}, λ_{max} = 402 nm) is a reactive anionic azo textile dye that was obtained from Tehranacid Company (Iran). Its chemical structure is illustrated in Figure 1. Low molecular weight chitosan, with the degree of deacetylation of 75-85%, and other common chemicals were all purchased from Sigma-Aldrich, and used without further purification. Double distilled water (DDW) was used to prepare all the solutions.

An appropriate volume of 0.1 M sodium hydroxide and hydrochloric acid solutions was used for carefully adjusting the pH of the dye solution, which was monitored by a pH meter.

Preparation of CS/$CoFe_2O_4$

In a typical procedure, 2.7 g $FeCl_3.6H_2O$ and 1.19 g $CoCl_2.6H_2O$ were dissolved in 40 mL DDW, followed by intensive sonication for 30 min to a homogeneous solution, which was denoted as 'solution A'. The chitosan solution was prepared by dissolving 0.8 g chitosan into 50 mL acetic acid (2% v/v). To prepare the CS/$CoFe_2O_4$ composite, the chitosan solution was slowly added to solution A. The temperature of the mixed solution was raised to 80 °C under simultaneous vigorous stirring. Subsequently, the pH of the solution was increased to 10.5, by adding droplets of 2M NaOH. Afterwards, 0.5 mL of 25 wt% glutaraldehyde was added as a cross-linking agent into the mixture. The resulting brownish red suspension was sealed in a Teflon-lined stainless-steel autoclave and maintained at 200 °C for 4 h in a furnace. The reaction product (CS/$CoFe_2O_4$ composite) was collected with the help of a magnet, rinsed with DDW and ethanol to remove residual chitosan and inorganic ions, and finally was dried at 60 °C for 10 h in a hot air oven. Naked $CoFe_2O_4$ particles were prepared by the same procedure without the addition of chitosan.

Characterization techniques

Fourier transform infrared (FTIR) spectra (400-4000 cm^{-1}) were recorded by a spectrometer (Vector 22, Bruker, USA) by the standard KBr pellet method. X-ray powder diffraction (XRD) patterns were obtained on an X-ray diffractometer (X'pert PRO, Panalytical) at a voltage of 40 kV and a current of 100 mA, with CuKα radiation (λ = 1.54056 Å). Field emission-electron microscopy (FESEM) images were recorded by using a scanning electron microscope (Sigma, Zeiss), operated at an acceleration voltage of 20.0 kV. Energy dispersive X-ray spectra (EDX) were also recorded. Thermogravimetric analysis (TGA) was conducted using a thermal analyzer (STA 1500, Rheometric Scientific, USA), where the samples were heated in the range of 10-800 °C at the rate of 10 °C min^{-1} under a N_2 atmosphere. The assessment of magnetization was performed by a vibrating-sample magnetometer (VSM, Meghnatis Kavir Kashan Co, Iran) at room temperature.

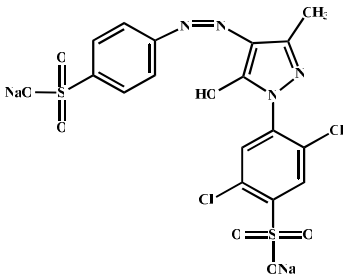

Figure 1: Chemical structure of Acid Yellow 17 (AY17) dye

Batch adsorption procedure

A typical batch adsorption experiment was conducted in the following way: 10 mg of CS/$CoFe_2O_4$ was added into 10 mL of AY17 solution with an initial dye concentration of 20 mg L^{-1} in a 25 mL Erlenmeyer flask, followed by mechanically agitating at 200 rpm for fixed various time. At the end of the adsorption process, the saturated CS/$CoFe_2O_4$ was separated by a hand-held magnet and the supernatant was immediately subjected to UV-Vis spectroscopy (Lambda 35 UV-Vis spectrophotometer, Perkin Elmer) at 402 nm to measure the concentration of AY17 in the remaining solution. A standard curve, used to convert absorbance data into concentrations for kinetic and

thermodynamic studies, was drawn to calculate the dye concentration in each adsorption experiment. The adsorption capacity (q_e, mg g^{-1}) and the removal percentage ($R(\%)$) were calculated using the following equations:

$$q_e = \frac{(C_0 - C_e)\,V}{M} \quad (1)$$

$$R(\%) = \frac{(C_0 - C_e)}{C_0} \times 100 \quad (2)$$

where q (mg g^{-1}) is the amount of AY17 adsorbed per unit amount of $CS/CoFe_2O_4$, C_0 (mg L^{-1}) is the initial concentration of AY17, M (g) is the mass of the $CS/CoFe_2O_4$, V (L) is the volume of AY17 solution, $R(\%)$ is the removal efficiency of AY17, and C_t (mg L^{-1}) is the concentration of AY17 at time t.

RESULTS AND DISCUSSION

Characterization of $CS/CoFe_2O_4$

FTIR spectra

Figure 2 (a, b and c) represents the spectra of pure chitosan, $CS/CoFe_2O_4$ and naked $CoFe_2O_4$ particles in the range of 400-4000 cm^{-1}, respectively. In Figure 2 (a), the broad and intense peaks near 3436 cm^{-1} for pure CS correspond to the characteristic absorption bands of the O–H bond, which was overlapped with the stretching vibrations of N–H. The peaks located at 1660, 1608, 1378 and 1085 cm^{-1} are attributed to the stretching vibrations of the C=O group of the –NH=C=O bond, the rocking vibrations of the N–H bond, stretching of C–OH, and stretching of C–O–C, respectively. The peak at 2881 cm^{-1} is ascribed to symmetric stretching vibrations in the CH_2 bond of chitosan.[13]

The FTIR spectrum of $CS/CoFe_2O_4$ shows two absorption bands at 3420 and 1624 cm^{-1}, which belong to the stretching vibrations of N–H of amine (and O–H) and scissoring vibrations of N–H of primary amine, respectively, appeared in the chitosan spectrum because of the free amine groups available in cross-linked chitosan. In addition, the typical peaks observed at around 418 and 580 cm^{-1} in the IR spectrum of $CS/CoFe_2O_4$ and naked $CoFe_2O_4$ particles (Fig. 2 (b) and (c)) correspond to the stretching vibrations of Co–O and Fe–O bonds in the ferrite lattice. After chitosan coating was applied on the surface of $CoFe_2O_4$, the vibrations of Fe–O become weaker in $CS/CoFe_2O_4$.[14]

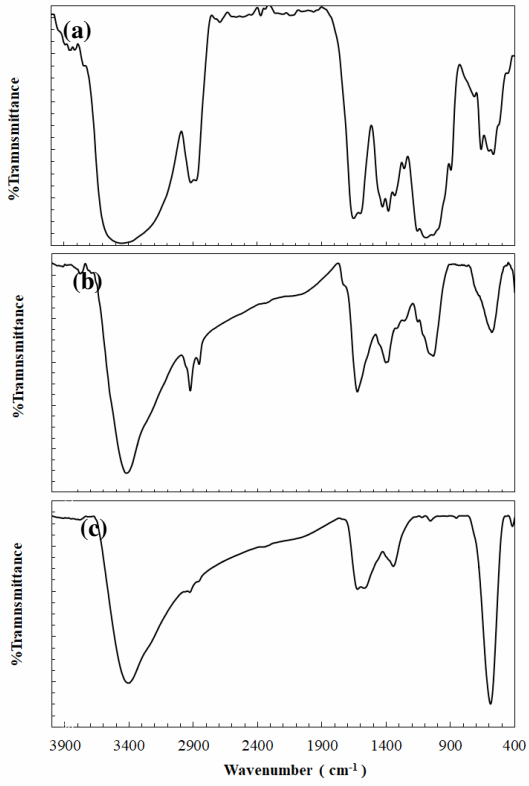

Figure 2: FTIR spectra of (a) CS, (b) $CS/CoFe_2O_4$, and (c) naked $CoFe_2O_4$

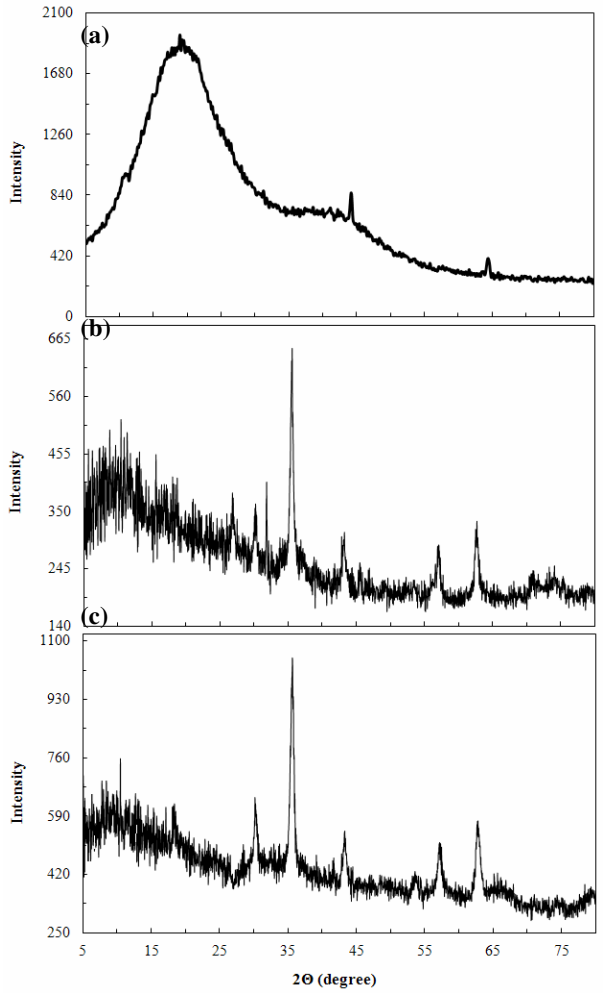

Figure 3: XRD patterns of (a) CS, (b) CS/$CoFe_2O_4$, and (c) naked $CoFe_2O_4$

XRD patterns

XRD patterns of pure chitosan, CS/$CoFe_2O_4$ and naked $CoFe_2O_4$ are shown in Figure 3 (a), (b) and (c), respectively. The broad peak appearing in Figure 3 (a) and (b), at the 2θ value of 20.5°, is due to the presence of chitosan with the amorphous state.[15] Seven main characteristic peaks, at 2θ of 18.3°, 30.2°, 35.5°, 43.2°, 45.5°, 57.0° and 62.6°, visible in Figure 3 (b) and (c), belong to (111), (220), (311), (400), (422), (511) and (440) crystalline plates of cobalt ferrite with a cubic spinel structure, according to JCPDS card No. 22-1086,[16,17] which are observed in both naked $CoFe_2O_4$ and $CoFe_2O_4$/CS. The sharp and strong peaks confirm that the two products were successfully prepared and well crystallized.[13]

Morphology

The morphology and the particle size distribution of the CS/$CoFe_2O_4$ were further analyzed by FE-SEM.[18] From the FE-SEM image depicted in Figure 4, the spherical shape of $CoFe_2O_4$ particles is clearly observed, with the estimated cluster size ranging between 30-80 nm. They are agglomerated to some extent on the relatively rough surface of chitosan.

EDX analysis

The EDX spectrum of CS/$CoFe_2O_4$ and the quantitative elemental composition shown in Figure 5 demonstrate the presence of C, O, N, Fe and Co elements in CS/$CoFe_2O_4$. The carbon and nitrogen signals originate from chitosan, while the

Co and Fe signals, with the atomic ratio of 1:2, come from the $CoFe_2O_4$ particles, which is evidence of $CoFe_2O_4$ in the composite.

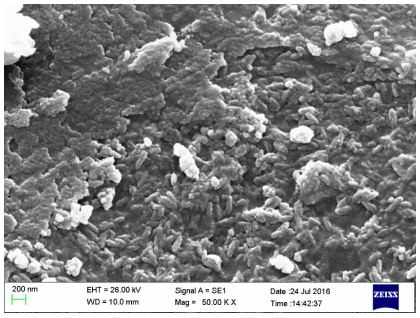

Figure 4: FE-SEM image of $CS/CoFe_2O_4$

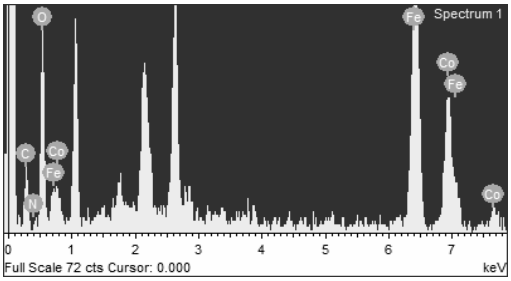

Element	Weight%	Atomic%
C K	19.26	31.99
N K	6.56	9.34
O K	36.44	45.44
Fe K	24.32	8.69
Co K	13.42	4.54

Figure 5: EDX pattern of $CS/CoFe_2O_4$ and its quantitative elemental composition

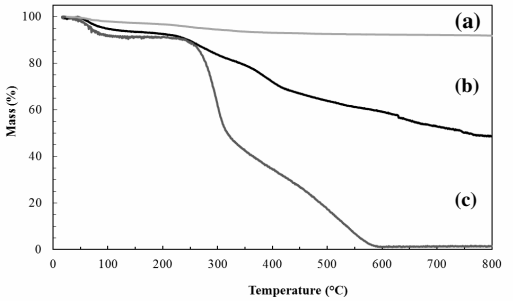

Figure 6: TGA thermograms of (a) naked $CoFe_2O_4$, (b) $CS/CoFe_2O_4$, and (c) CS

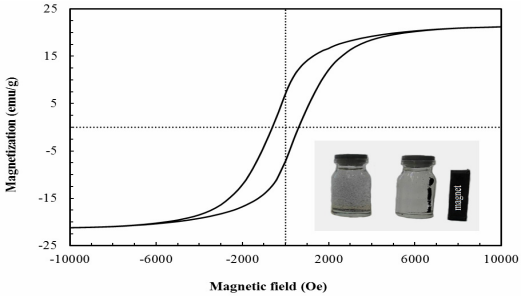

Figure 7: Magnetic hysteresis curve for $CS/CoFe_2O_4$. Inset displays a photograph of $CS/CoFe_2O_4$ dispersion in solution and magnetic separation from solution

TGA analysis

The TGA results for naked $CoFe_2O_4$, $CS/CoFe_2O_4$ composite and pure CS, under nitrogen, are shown in Figure 7 (a), (b) and (c), respectively. The curve of naked $CoFe_2O_4$ in Figure 6 (a) exhibits no remarkable peaks. The initial mass loss of $CoFe_2O_4$ below 200 °C is of about 3.1%, which is attributed to the loss of physically adsorbed moisture. The mass loss of 5.2% occurring from 200 to 800 °C can be ascribed to the loss of residual solvents used in the synthesis process.[19] For $CS/CoFe_2O_4$ in Figure 6 (b), the mass loss is around 9% below 200 °C, similarly owing to the removal of adsorbed water molecules through physical and chemical interactions, but the considerable degradation observed between 200 °C and 570 °C corresponds to the breakdown of the main CS chains coating the magnetic particles. Beyond 570 °C, no significant change is observed in the mass,

indicating the presence of ferrite cobalt above this temperature. For CS in Figure 6 (c), nearly 9% loss of CS mass is observed at temperatures lower than 200 °C, resulting from evaporation of adsorbed moisture. The decomposition of acetylated and deacetylated units of CS occurring at 250-450 °C causes the main mass loss of CS.[15,20] According to the TGA curves, the CS content of the CS/$CoFe_2O_4$ composite is estimated to be about 40%. The introduction of $CoFe_2O_4$ particles into the CS polymer decreases its crystallinity. The results of TGA further confirmed that the $CoFe_2O_4$ particles were successfully coated with the CS polymer, supporting the findings of the FTIR and EDX analyses.

Magnetic property

The magnetic behavior of CS/$CoFe_2O_4$ was analyzed at room temperature with applied magnetic field sweeping from –10 to +10 kOe and the result is shown in Figure 7. It was observed that an increase in the external magnetic field reinforces magnetization of CS/$CoFe_2O_4$ and its saturation magnetization value (M_s) reaches 21.21 emu g^{-1}. Comparatively, this is lower than that reported for bare $CoFe_2O_4$ (49.55 emu g^{-1}).[18] The decreased saturation magnetization was most likely attributed to the presence of the non-magnetic chitosan coating on the surface of $CoFe_2O_4$ particles.[21] The insert of Figure 7 indicates that CS/$CoFe_2O_4$ can be conveniently attracted and separated from an aqueous solution by a hand-held magnet beside the vial.

pH at point of zero charge

The pH_{pzc} (pH at the point of zero charge, *i.e.* the pH at which the electric charge density of the adsorbent surface is zero) is a critical parameter for explaining the efficacy of the adsorption process concerning the electrostatic interactions between adsorbent and adsorbate materials.[15] The pH_{pzc} of CS/$CoFe_2O_4$ was measured by mixing 0.02 g of CS/$CoFe_2O_4$ and 25 mL of 0.1 mol^{-1} sodium chloride electrolyte solution in the initial pH range of 2.5-9.0 at 298 K, with continuous stirring at 200 rpm for 24 h. Figure 8 shows the curve of ΔpH [pH_{intial}-pH_{funal}] *versus* $pH_{initial}$. The pH_{pzc} was estimated to be 6.8.

Adsorption studies

Effect of initial solution pH

The pH may be one of the key factors controlling the adsorption of pollutants onto adsorbents.[22] As seen in Figure 9 (a), the adsorption process was strongly dependent on pH. The highest dye removal efficiency (83%) was found to be at the initial pH 4.0. This phenomenon can be attributed to the enhanced electrostatic attractions between the negatively charged AY17 dye anions and the positively charged surface of CS/$CoFe_2O_4$ at lower pH values. Two sulfonate groups ($-SO_3^-$) of AY17 (shown in Fig. 1) are readily dissociated and have negative charges in aqueous solution. The amine groups($-NH_2$) of chitosan molecules on the surface of CS/$CoFe_2O_4$ can be protonated as a form of $-NH_3^+$. Therefore, the adsorption mechanism of the acidic dye (Dye$-SO_3^-Na^+$) is presented in the following equation:[23]

$$R-NH^+ + H^+ \rightleftharpoons R-NH_3^+ \quad (3)$$

$$Dye-SO_3^-\,Na^+ \xrightleftharpoons{H_2O} Dye-SO_3^- + Na^+ \quad (4)$$

$$R-NH_3^+ + Dye-SO_3^-\,Na^+ \rightleftharpoons R-NH_3^+\,{}^-O_3S-Dye \quad (5)$$

where R is the alkyl group of the original form of chitosan in the CS/$CoFe_2O_4$.

In extremely acidic pH ranges (less than the optimum pH value of 4.0), dye dissociation decreases, leading to a lower concentration of the anionic dye species available to interact with the positively charged sites of CS/$CoFe_2O_4$.

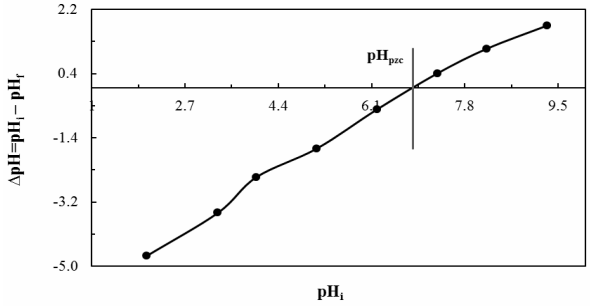

Figure 8: pH point of zero charge of CS/$CoFe_2O_4$

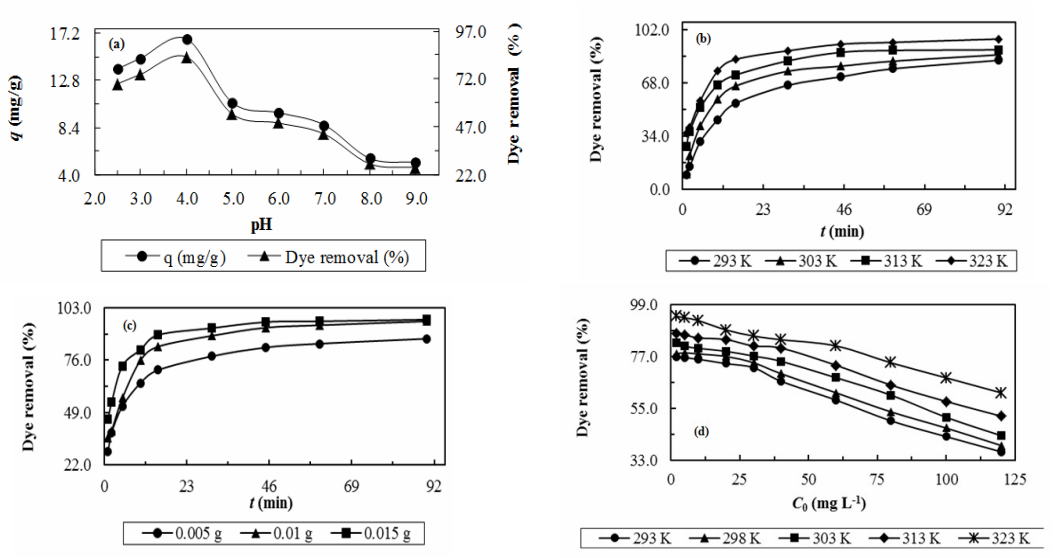

Figure 9: Parameters affecting AY17 removal efficiency: (a) initial solution pH, (b) temperature and contact time, (c) CS/$CoFe_2O_4$ adsorbent dosage and contact time, and (d) initial AY17 dye concentration

Therefore, the dye removal efficiency reduced at pH < 4.0. The point of zero charge for CS/$CoFe_2O_4$ was found to be 6.8. Therefore, the surface charge of the CS/$CoFe_2O_4$ is positive at pH < 6.8, which is favorable for the adsorption of an anionic dye.

However, at a pH above 6.8, the CS/$CoFe_2O_4$ has negative surface potential, which increases repulsion between its surface and AY17. Additionally, more OH^- ions are available to compete with the anionic sulfonate groups in alkaline medium, thereby AY17 removal efficiency decreases significantly.[24] In summary, the optimum pH value for AY17 adsorption was determined to be 4.0. All subsequent adsorption experiments were conducted at the optimum pH value. The inset of Figure 9 (a) shows a photographic image of AY17 solution before (left) and after (right) adsorption onto 0.01 g CS/$CoFe_2O_4$ at pH 4.0 and 323 K. Obviously, the color of the solution disappeared after treatment with the adsorbent.

Effect of temperature and contact time

The contact time between adsorbent and adsorbate is another significant parameter for evaluating the adsorption properties of adsorbents. Figure 9 (b) illustrates the impact of contact time on AY17 removal efficiency (%) at various temperatures. The trend of the curves is similar to those described in other studies reported in the literature. Initially, the removal efficiency increased sharply. After a while, it rose mildly with further increase of contact time and steadily at equilibrium time. The rapid adsorption at first may be due to the abundant availability of active sites on CS/$CoFe_2O_4$ and the AY17 anion dyes interact easily with the adsorption sites, while the following slower rate can be explained by the exhaustion of the open adsorptive sites and by the repulsion between the dye anions and the bulk phases, which hindered the binding of AY17 to the remaining active sites.[15]

AY17 removal efficiency in 45 min at temperatures of 293, 303, 313 and 323 K was 72%, 78%, 87% and 92%, respectively (Fig. 9 (b)). Obviously, an increase in the temperature led to an enhancement in dye removal efficiency. Therefore, AY17 adsorption onto CS/$CoFe_2O_4$ was endothermic. Moreover, with increasing the temperature, the adsorption process reached equilibrium more quickly. It seems that not only the number of adsorptive sites augments at a higher temperature, but also the penetration of dye anions into the possible surface cavities is facilitated.[25]

Effect of CS/$CoFe_2O_4$ dosage and contact time

The dye removal efficiency is significantly influenced by the amount, size and pore volume of the adsorbent, showing its cost-effectiveness in the adsorption processes.[26] The plot of AY17

removal efficiency (%) *versus* time (min) at various CS/$CoFe_2O_4$ doses (g) is shown in Figure 9 (c). It was found that removal efficiency increased with an increasing initial amount of CS/$CoFe_2O_4$. It can be ascribed to the increase in the surface area of the adsorbent, as well as the abundant accessibility of adsorptive sites in spite of the fixed finite number of dye anions.[27] The smooth enhancement in the AY17 removal efficiency at a higher adsorbent amount can be due to decreasing the unit contact area between AY17 and CS/$CoFe_2O_4$, as well as the diffusion path length resulting from overlapping or aggregation of the adsorptive sites. The removal efficiency in 60 min was found to be 84%, 94% and 96% for 0.005, 0.01 and 0.015 g of CS/$CoFe_2O_4$, respectively. However, a dose of 0.01 g was used for subsequent experiments.

Effect of initial AY17 dye concentration

The initial dye concentration plays a predominant role in color removal. Figure 9 (d) illustrates the effect of initial AY17 concentration on color removal by CS/$CoFe_2O_4$ at several temperatures. As seen from Figure 9 (d), AY17 removal efficiency fell from 78% to 36% as the initial AY17 concentration increased from 2 to 120 mg L^{-1} at 293 K. The reduction of dye removal efficiency may be due to the fact that at the higher initial dye concentration, the total exiting adsorptive sites are confined as a result of the fixed amount of adsorbent. Hence, saturation of the adsorptive sites of the adsorbent with dye anions may occur as the adsorption process continues,[28] leading to a decrease in dye removal with an increase in dye concentration. Furthermore, from Figure 9 (d), it is observed that the removal efficiency improved from 36% at 293 K to 61% at 323 K at an initial concentration of 120 mg L^{-1}.

Adsorption kinetics

The study of adsorption kinetics is necessary for wastewater treatment using adsorbents since it provides highly valuable information on reaction pathways and the mechanisms controlling the adsorption process, such as chemical reaction, mass transfer and diffusion,[29] which is helpful in designing an effective and fast model for the adsorption of colored pollutants. Hence, five common kinetic models were employed to fit the kinetic adsorption data of AY17 dye onto CS/$CoFe_2O_4$ by the non-linear method using Mathematica 9.0 software, that is, the Lagergren pseudo-first order,[30] pseudo-second order,[31] intraparticle diffusion,[32] simplified Elovich,[33] and fractional power[34] models. The mathematical equations for these models are given in Table 1, where q_e (mg g^{-1}) and q_t (mg g^{-1}) are the adsorption capacity at equilibrium and any time *t*, respectively; k_1 (min^{-1}) and k_2 (g mg^{-1} min^{-1}) are the pseudo-first order and pseudo-second order constant, respectively; k_i ($mg\,g^{-1}min^{-1/2}$) is the intraparticle diffusion rate constant; C ($mg\,g^{-1}$) is a constant related to boundary layer thickness; α ($mg\,g^{-1}min^{-1}$) is the initial adsorption rate constant; β ($g\,mg^{-1}$) is the desorption constant; a($mg\,g^{-1}min^{-b}$)is the fractional power rate constant; b is the power of the fractional power model. The parameters of the kinetic models, along with the correlation coefficients (R^2) resulted by fitting the models to experimental data at temperatures of 293, 303, 313 and 323 K were summarized in Table 1. The non-linear plots of the kinetics models of AY17 adsorption are shown in Figure 10.

As can be seen from Table 1, the correlation coefficients obtained from the pseudo-second order model are above 0.997, higher than those of the other models. In addition, compared with the pseudo-first order model, the values of q_e calculated using the pseudo-second order model are more consistent with the experimental values of q_e, given in the last row of Table 1, for all the temperatures studied. Based on these results, the pseudo-second order model described better the kinetic adsorption behavior of AY17 onto the CS/$CoFe_2O_4$ magnetic composite. As seen in Table 1, the values of the pseudo-second order constant, k_2, decreased from 0.0056 g mg^{-1} min^{-1} to 0.0189 g mg^{-1} min^{-1} with the increase in temperature from 293 K to 323 K. Meanwhile, the calculated q_e improved from 17.97 mg g^{-1} at 293 K to 19.47 mg g^{-1} at 323 K. In fact, with the rise in temperature, the diffusion of AY17 anions into the pores of the CS/$CoFe_2O_4$ adsorbent was facilitated. Besides, more AY17 anions gained sufficient kinetic energy for interaction with the adsorptive active sites of CS/$CoFe_2O_4$, resulting in an enhancement of the adsorption rate.

Activation energy of adsorption

The activation energy of AY17 adsorption onto CS/$CoFe_2O_4$ was calculated from the rate constants (k_2) obtained for the experiments conducted in the range of 293-323 K.

Table 1
Non-linear kinetic parameters for AY17 adsorption onto $CS/CoFe_2O_4$ at various temperatures*

Kinetic models	Parameters	Temperature (K)			
		293	303	313	323
Pseudo-first order	$k_1\ (\mathrm{min^{-1}})$	0.0872	0.1277	0.2140	0.2465
$q_t = q_e(1-e^{-k_1 t})$	$q_{e,cal}\ (\mathrm{mg\,g^{-1}})$	15.3428	16.1513	16.8312	18.0335
	R^2	0.9968	0.9981	0.9918	0.9913
Pseudo-second order	$k_2\ (\mathrm{g\,mg^{-1}min^{-1}})$	0.0056	0.0087	0.0169	0.0189
$q_t = \frac{k_2 q_e^2 t}{1+k_2 q_e t}$	$q_{e,cal}\ (\mathrm{mg\,g^{-1}})$	17.9709	18.266	18.3228	19.4722
	R^2	0.9997	0.9995	0.9985	0.9973
Intraparticle diffusion	$k_i\ (\mathrm{mg\,g^{-1}min^{-1/2}})$	1.7476	1.7018	1.4330	1.4279
$q_t = k_i t^{0.5} + C$	$C\ (\mathrm{mg\,g^{-1}})$	2.0589	3.7172	6.8762	8.1967
	R^2	0.9821	0.9707	0.9833	0.9833
Simplified Elovich	$\alpha\ (\mathrm{mg\,g^{-1}min^{-1}})$	4.8117	7.0525	21.0018	32.2607
$q_t = \frac{1}{\beta}\ln(\alpha\beta) + \frac{1}{\beta}\ln t$	$\beta\ (\mathrm{g\,mg^{-1}})$	0.2885	0.2840	0.3372	0.3365
	R^2	0.9984	0.9966	0.9979	0.9965
Fractional power	$a(\mathrm{mg\,g^{-1}min^{-b}})$	3.5569	4.8840	7.2483	8.4204
	b	0.3593	0.3019	0.2217	0.2022
$q_t = a\,t^b$	R^2	0.9892	0.9826	0.99209	0.9924
	$q_{e,exp}\ (\mathrm{mg\,g^{-1}})$	16.4948	17.1915	17.8423	19.2132

*Experimental conditions: pH 4.0, 0.01 g of $CS/CoFe_2O_4$, 10 mL of 20.0 mg L^{-1} of AY17 solution

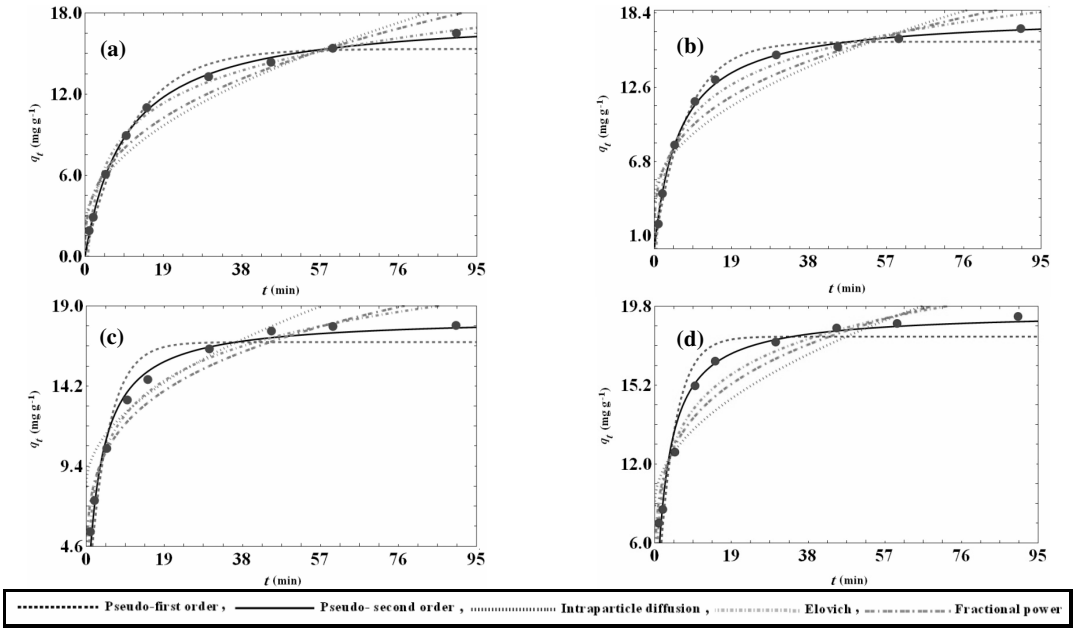

Figure 10: Non-linear plots of kinetic models for the adsorption of AY17 onto $CS/CoFe_2O_4$ at temperatures of (a) 293, (b) 303, (c) 313, (d) 323 K (black circles show experimental data; experimental conditions: pH 4.0, 0.01 g of $CS/CoFe_2O_4$, 10 mL of 20.0 mg L^{-1} of AY17 solution)

The Arrhenius equation was used for this purpose:

$$k_2 = A\,e^{-\frac{E_a}{RT}} \quad (6)$$

where $k_2\ (\mathrm{g\,mg^{-1}min^{-1}})$ is the rate constant for the pseudo-second-order kinetic model; $A\ (\mathrm{g\,mg^{-1}min^{-1}})$ is the temperature-independent Arrhenius factor; $E_a\ (\mathrm{J\,mol^{-1}})$ is the activation energy, $R\ (8.314\ \mathrm{J\,mol^{-1}\,K^{-1}})$ is the universal gas constant, and $T\ (\mathrm{K})$ is temperature.

The magnitude of activation energy may provide evidence about the physical or chemical nature of the adsorption process. The physical adsorption normally has a low activation energy (5-50 $\mathrm{kJ\,mol^{-1}}$), while chemical adsorption has a

high activation energy (60-800 $\mathrm{kJ\,mol^{-1}}$).[35] The obtained value of E_a, 29.66 $\mathrm{kJ\,mol^{-1}}$, for the adsorption of AY17 onto CS/$CoFe_2O_4$ was within the range of physisorption.

Adsorption isotherms

Adsorption isotherms can describe surface properties and the affinity of an adsorbent, which are effective factors on the interactive behavior between adsorbent and adsorbate materials, aiding the design of a desired adsorption system. Five well-known adsorption isotherms, namely Langmuir,[36] Freundlich,[37] Dubinin-Radushkevich,[38] Temkin[39] and Jovanovic,[40] were employed here to fit with the adsorption isotherm data of AY17 onto CS/$CoFe_2O_4$ and naked $CoFe_2O_4$, using the non-linear method. The equation of the tested models are given in Table 2, where q_m $(\mathrm{mg\,g^{-1}})$ is the maximum adsorption capacity of the adsorbent to generate a single layer; K_L $(\mathrm{L\,mg^{-1}})$ is the Langmuir isotherm constant associated with free energy and the affinity of adsorption, K_F $(\mathrm{mg^{1-\frac{1}{n}}\,L^{\frac{1}{n}}\,g^{-1}})$ and n are Freundlich isotherm constants, indicating the adsorption capacity; n is the heterogeneity factor, related to adsorption capacity; q_s $(\mathrm{mg\,g^{-1}})$ is the Dubinin-Radushkevich constant related to the degree of dye adsorption; $k_{ad}(\mathrm{mol^2\,J^{-2}})$ is the Dubinin-Radushkevich isotherm constant related to sorption energy; ε is known as the Polanyi potential whose value is represented by the following equation:

$$\varepsilon = RT\ln\left[1+\frac{1}{C_e}\right] \quad (7)$$

b_T $(\mathrm{J\,g\,mol^{-1}\,mg^{-1}})$ is the Temkin isotherm constant; A_T $(\mathrm{L\,mg^{-1}})$ is the equilibrium binding constant.

The isothermal parameters and the correlation coefficients (R^2) were summarized at temperatures of 293 K, 298 K, 303 K, 313 K and 323 K for CS/$CoFe_2O_4$ and at 323 K for naked $CoFe_2O_4$. The non-linear plots of the isotherm models are shown in Figure 11 ((a)-(f)). It can be seen from Table 2 that the Langmuir isotherm has better conformity with the experimental data due to the correlation coefficient, R^2, higher than 0.995, indicating that the AY17 dye uptake takes place on a homogeneous adsorbent by monolayer coverage without any interaction between AY17 anions. The calculated value for maximum adsorption capacity, q_m, of CS/$CoFe_2O_4$ increases from 51.98 mg g^{-1} to 89.10 mg g^{-1} with increasing temperature from 293 K to 323 K (Table 2). Therefore, higher temperature is beneficial to the adsorption process. In the last two columns of Table 2, the q_m values of CS/$CoFe_2O_4$ and naked $CoFe_2O_4$, obtained from the Langmuir model, were compared under the same experimental conditions. The q_m of CS/$CoFe_2O_4$ at 323 K and pH = 4.0 is 89.10, which is 226% higher than that of naked $CoFe_2O_4$, 27.31 mg g^{-1}. The result shows that the coating of $CoFe_2O_4$ with chitosan (which has plenty of hydroxyl and amino groups on the chain to connect to dye anions) remarkably improves its affinity to AY17.

The feasibility of the adsorption process is determined by a dimensionless constant separation factor, R_L, which is given as:

$$R_L = \frac{1}{1+K_L C_0} \quad (8)$$

where K_L $(\mathrm{L\,mg^{-1}})$ is the Langmuir equilibrium constant, C_0 is the highest initial concentration of dye. R_L values between 0 and 1 imply a desirable process, values larger than 1 are an indication of an unfavorable isotherm, and values equal to zero point out a totally irreversible isotherm.[41] For AY17 uptake onto CS/$CoFe_2O_4$, the separation factors, R_L, are less than 0.1 (Table 2). It is obvious that adsorption under the studied conditions is favorable.

Adsorption thermodynamics

The adsorption thermodynamic parameters, including changes in standard Gibb's free energy (ΔG°, J mol^{-1}), enthalpy (ΔH°, J mol^{-1}) and entropy (ΔS°, J mol^{-1} K^{-1}), for the adsorption of AY17 onto CS/$CoFe_2O_4$ were calculated using classical Equations (9) and (10):

$$\Delta G^\circ = \Delta H^\circ - T\Delta S^\circ \quad (9)$$

$$\Delta G^\circ = -RT\ln(K_L) \quad (10)$$

where R $(8.314\,\mathrm{J\,mol^{-1}\,K^{-1}})$ is the universal gas constant, T (K) is the absolute temperature, K_L $(\mathrm{L\,mg^{-1}})$ is the equilibrium constant obtained from the Langmuir equation and is the Langmuir constant. The values of ΔH° and ΔS° were calculated from the Van't Hoff non-linear plot of K_L against T. All the thermodynamic parameters are tabulated in Table 3.

Table 2
Non-linear isothemal parameters for the adsorption of AY17 onto CS/$CoFe_2O_4$ at various temperatures*

Isotherm models	Parameters	CS/CoFe2O4					CoFe2O4
		Temperature (K)					
		293	298	303	313	323	323
Langmuir	q_m (mg g^{-1})	51.9805	56.2245	63.1845	72.5804	89.1014	27.3132
$q_e = \frac{q_m K_L C_e}{1 + K_L C_e}$	K_L (L mg^{-1})	0.0795	0.0820	0.0873	0.0947	0.1012	0.1061
	R_L	0.0949	0.0922	0.0871	0.0809	0.0761	0.0728
	R^2	0.9996	0.9996	0.9988	0.9997	0.9990	0.9967
Freundlich	K_F (mg$^{1-\frac{1}{n}}$ L$^{\frac{1}{n}}$ g^{-1})	7.7770	8.443	9.7751	11.1091	11.1147	5.8638
$q_e = K_F C_e^{1/n}$	n	2.3611	2.3429	2.3480	2.2599	1.8432	2.9545
	R^2	0.9850	0.9848	0.9804	0.9880	0.9900	0.9944
Dubinin-Radushkevich	q_s (mg g^{-1})	40.4226	43.3696	49.0375	55.2929	66.2438	23.557
$q_e = q_s e^{-K_{ad}\varepsilon^2}$	k_{ad} (mol^2 kJ^{-2})	7.2330	6.2295	5.6944	3.9857	3.2766	8.6862
	R^2	0.9809	0.9789	0.9824	0.9770	0.9729	0.9682
Temkin	A_T (L mg^{-1})	1.3967	1.4663	1.6633	2.0433	3.7419	3.0440
$q_e = \frac{R\,T}{b_T} \ln A_T C_e$	b_T (J g mol^{-1} mg^{-1})	259.383	245.246	227.234	211.901	208.796	610.188
	R^2	0.9907	0.9903	0.9849	0.9846	0.9702	0.9952
Jovanovic	q_m (mg g^{-1})	42.8862	46.3275	51.95	59.2165	71.6038	24.0159
$q_e = q_m(1 - e^{K_J C_e})$	K_J (L mg^{-1})	–0.0759	–0.0784	–0.0846	–0.0931	–0.1017	–0.0799
	R^2	0.9989	0.9989	0.9999	0.9979	0.9974	0.9914

*Experimental conditions: pH 4.0, 0.01 g of adsorbent, 10 mL of AY17 solution, contact time of 60 min

Table 3
Thermodynamic parameters for the adsorption of AY17 onto CS/$CoFe_2O_4$

Temperature (K)	ΔH (kJ mol^{-1})	ΔS (J mol^{-1}K^{-1})	$T\,\Delta S$ (kJ mol^{-1})	$-\Delta G$ (kJ mol^{-1})
293	6.4936	58.5183	17.1547	10.6610
298			17.4473	10.9536
303			17.7399	11.2462
313			18.3250	11.8314
323			18.9102	12.4166

The positive value of ΔH° confirmed the endothermic nature of adsorption, which was supported by the fact that the adsorption of AY17 increased at elevated temperatures. The ΔH° value (6.4936 J mol^{-1}) was less than 40 kJ mol^{-1}, thereby implying that the adsorption is predominantly physisorption.[42] The positive values of ΔS° implied an increased randomness at the solid/solution interface during dye uptake, indicating that the adsorption was entropy-driven.[43] The negative values of ΔG° suggested that the adsorption follows a spontaneous and thermodynamically feasible trend under the experimental conditions, ΔG° value was more negative with the rise in temperature, showing that higher temperature will facilitate the adsorption of AY17 dyes onto $CS/CoFe_2O_4$.

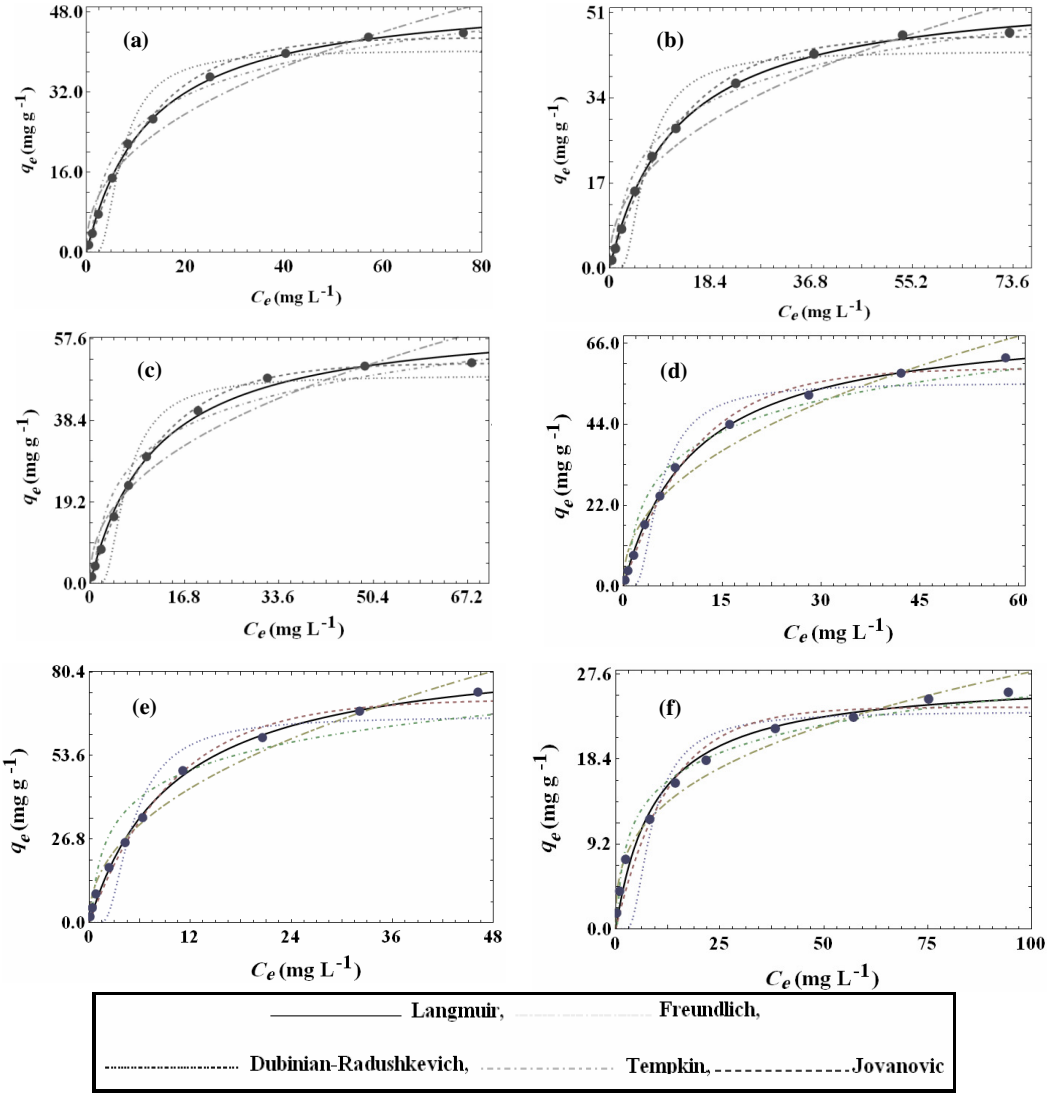

Figure 11: Non-linear plots of isotherm models for the adsorption of AY17 onto $CS/CoFe_2O_4$ at temperatures of (a) 293, (b) 298, (c) 303, (d) 313, (e) 323 K and onto naked $CoFe_2O_4$ at the temperature of (f) 323 K (black circles show experimental data; experimental conditions: pH 4.0, 0.01 g of $CS/CoFe_2O_4$, 10 mL of AY17 solution, contact time of 60 min)

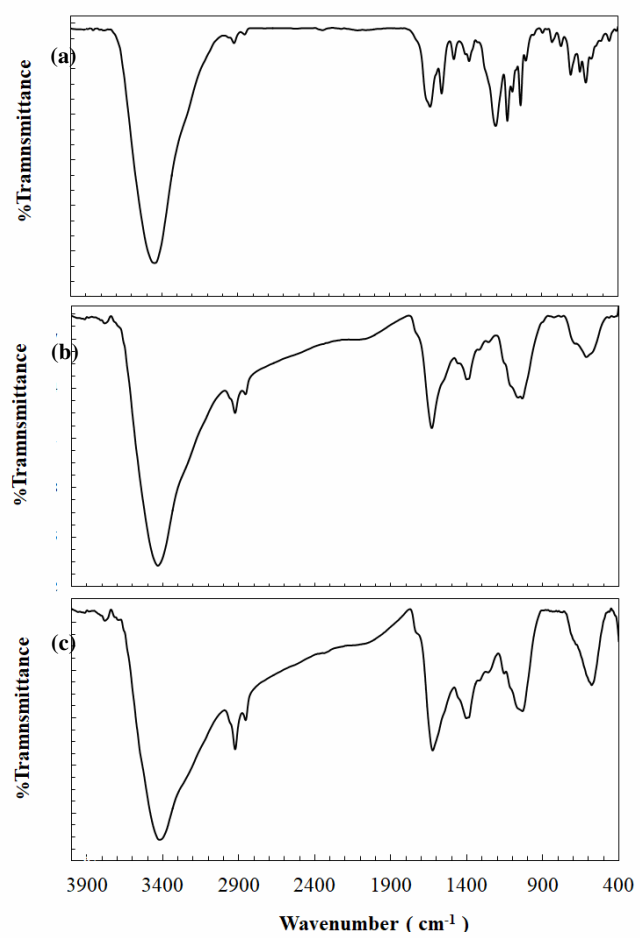

Figure 12: FTIR spectra of AY17 (a) before and (b) after adsorption onto (c) $CS/CoFe_2O_4$

Analysis of adsorption mechanism

The FTIR analysis was carried out to identify possible active sites on the $CS/CoFe_2O_4$ magnetic composite for bonding of the AY17 dye. The FTIR spectra of AY17 (a) before and (b) after adsorption are illustrated in Figure 12 (a) and (b), respectively.

The intensity of the strong bands located in the range of 1100-1380 cm^{-1}, attributed to symmetric and asymmetric stretching vibrations of S=O of AY17, markedly decreased after adsorption onto $CS/CoFe_2O_4$ (Fig. 12 (b)), while some peaks entirely disappeared, indicating strong interactions between the SO_3^- groups of AY17 with the N–H groups of chitosan in $CS/CoFe_2O_4$. The peak around 3421 cm^{-1}, assigned to the O–H and N–H stretching vibrations in the FTIR spectrum of $CS/CoFe_2O_4$ (Fig. 12 (c)), was found to shift to 3433 cm^{-1} after AY17 adsorption (Fig. 12 (b)). Another change was observed with regard to the peak at 580 cm^{-1} (Fig. 12 (c)), which shifted toward 604 cm^{-1} after AY17 adsorption (Fig. 12 (b)), thereby confirming that $CoFe_2O_4$ inside $CS/CoFe_2O_4$ not only provides effective magnetic separation performance, but also behaves as a binding site for dye adsorption.[12]

Based on the results obtained in this work, electrostatic interactions and the formation of hydrogen bonding are possible mechanisms of dye adsorption onto $CS/CoFe_2O_4$. Moreover, the pore structure of the adsorbent is beneficial to the diffusion of AY17 anions.

CONCLUSION

The $CS/CoFe_2O_4$ magnetic composite was successfully prepared. It possessed excellent adsorption properties for effective removal of a hazardous dye, Acid Yellow 17, and suitable magnetic characteristics, of 21.2 emu g^{-1}, which make the magnetic composite recyclable for further adsorption applications. The pseudo-second order kinetic model with its high

correlation was appropriate to describe the kinetic process of AY17 uptake onto CS/$CoFe_2O_4$. The Langmuir model fitted the adsorption data, suggesting the homogeneity of active sites on the surface of $CoFe_2O_4$/CS. The maximum adsorption capacity of CS/$CoFe_2O_4$ obtained from the Langmuir model was 89.10 mg g^{-1} at 323 K, which was much higher than that of naked $CoFe_2O_4$, 27.31 mg g^{-1}. Based on the thermodynamic parameters, the adsorption process was a spontaneous, favorable and endothermic process in nature.

REFERENCES

[1] M. T. Yagub, T. K. Sen, S. Afroze and H. M. Ang, *Adv. Colloid Interface Sci.*, **209**, 172 (2014).

[2] V. K. Gupta and Suhas, *J. Environ. Manage.*, **90**, 2313 (2009).

[3] K. A. Adegoke and O. S. Bello, *Water Resour. Ind.*, **12**, 8 (2015).

[4] K. B. Tan, M. Vakili, B. A. Horri, P. E. Poh, A. Z. Abdullah *et al.*, *Sep. Purif. Technol.*, **150**, 229 (2015).

[5] H. Fallah Moafi, R. Ansari and S. Sadeghinia, *Cellulose Chem. Technol.*, **52**, 271 (2018).

[6] V. S. Munagapati and D.-S. Kim, *Ecotoxicol. Environ. Saf.*, **141**, 226 (2017).

[7] K. K. Kefeni, B. B. Mamba and T. A. M. Msagati, *Sep. Purif. Technol.*, **188**, 399 (2017).

[8] R. Sivashankar, A. B. Sathya, K. Vasantharaj and V. Sivasubramanian, *Environ. Nanotechnol. Monit. Manag.*, **1**, 36 (2014).

[9] X. Zhao, L. Lv, W. Zhang, S. Zhang and Q. Zhang, *Chem. Eng. J.*, **170**, 381 (2011).

[10] D. H. K. Reddy and S.-M. Lee, *Adv. Colloid Interface Sci.*, **201–202**, 68 (2013).

[11] A. Z. M. Badruddoza, Z. B. Z. Shawon, W. J. D. Tay, K. Hidajat and M. S. Uddin, *Carbohyd. Polym.*, **91**, 322 (2013).

[12] X. Li, H. Lu, Y. Zhang, F. He, L. Jing *et al.*, *Appl. Surf. Sci.*, **389**, 567 (2016).

[13] Y. Zhang, T. Yan, L. Yan, X. Guo, L. Cui *et al.*, *J. Mol. Liq.*, **198**, 381 (2014).

[14] C. Ren, X. Ding, H. Fu, C. Meng, W. Li *et al.*, *RSC Adv.*, **6**, 72479 (2016).

[15] A. S. K. Kumar and S.-J. Jiang, *J. Environ. Chem. Eng.*, **4**, 1698 (2016).

[16] L. Wang, J. Li, Y. Wang, L. Zhao and Q. Jiang, *Chem. Eng. J.*, **181**, 72 (2012).

[17] C. Fan, K. Li, J. Li, D. Ying, Y. Wang *et al.*, *J. Hazard. Mater.*, **326**, 211 (2017).

[18] C. Santhosh, P. Kollu, S. Felix, V. Velmurugan, S. K. Jeong *et al.*, *RSC Adv.*, **5**, 28965 (2015).

[19] L. Zhou, L. Ji, P.-C. Ma, Y. Shao, H. Zhang *et al.*, *J. Hazard. Mater.*, **265**, 104 (2014).

[20] N. A. Kalkan, S. Aksoy, E. A. Aksoy and N. Hasirci, *J. Appl. Polym. Sci.*, **124**, 576 (2012).

[21] Y. Xiao, H. Liang and Z. Wang, *Mater. Res. Bull.*, **48**, 3910 (2013).

[22] H. Zhu, Y. Fu, R. Jiang, J. Yao, L. Liu *et al.*, *Appl. Surf. Sci.*, **285**, 865 (2013).

[23] L. Zhou, J. Jin, Z. Liu, X. Liang and C. Shang, *J. Hazard. Mater.*, **185**, 1045 (2011).

[24] M. Ashrafi, M. Arab Chamjangali, G. Bagherian and N. Goudarzi, *Spectrochim. Acta Part A Mol. Biomol. Spectrosc.*, **171**, 268 (2017).

[25] N. A. Travlou, G. Z. Kyzas, N. K. Lazaridis and E. A. Deliyanni, *Langmuir*, **29**, 1657 (2013).

[26] S. Hajati, M. Ghaedi, F. Karimi, B. Barazesh, R. Sahraei *et al.*, *J. Ind. Eng. Chem.*, **20**, 564 (2014).

[27] S. Yavari, N. M. Mahmodi, P. Teymouri, B. Shahmoradi and A. Maleki, *J. Taiwan Inst. Chem. Eng.*, **59**, 320 (2016).

[28] O. A. Oyetade, V. O. Nyamori, B. S. Martincigh and S. B. Jonnalagadda, *RSC Adv.*, **5**, 22724 (2015).

[29] R. Sahraei, K. Hemmati and M. Ghaemy, *RSC Adv.*, **6**, 72487 (2016).

[30] S. Lagergren, *Sven. Veten. Handl.*, **24**, 1 (1898).

[31] Y. Ho and G. McKay, *Process Biochem.*, **34**, 451 (1999).

[32] J. C. Weber and W. J. Morris, *J. Sanit. Eng. Div.*, **89**, 31 (1963).

[33] S. H. Chien and W. R. Clayton, *Soil Sci. Soc. Am. J.*, **44**, 265 (1980).

[34] G. Limousin, J.-P. Gaudet, L. Charlet, S. Szenknect, V. Barthès *et al.*, *Appl. Geochem.*, **22**, 249 (2007).

[35] F. Deniz and S. D. Saygideger, *Bioresour. Technol.*, **101**, 5137 (2010).

[36] I. Langmuir, *J. Am. Chem. Soc.*, **40**, 1361 (1918).

[37] H. M. F. Freundlich, *Z. Phys. Chem.*, **57**, 385 (1906).

[38] L. V. Dubinin and M. M. Radushkevich, *Proc. Acad. Sci. USSR Phys. Chem. Sect.*, **55**, 331 (1947).

[39] V. Temkin and M. I. Pyzhev, *Acta Phys. Chim. USSR*, **12**, 327 (1940).

[40] D. S. Jovanović, *Kolloid-Zeitschrift Zeitschrift für Polym*, **235**, 1203 (1969).

[41] M. Ignat, V. Dulman and T. Onofrei, *Cellulose Chem. Technol.*, **46**, 357 (2012).

[42] F. Shakib, A. Dadvand Koohi and A. Kamran Pirzaman, *Water Sci. Technol.*, **75**, 1932 (2017).

[43] D. Suteu, T. Malutan and D. Bilba, *Cellulose Chem. Technol.*, **45**, 5 (2011).